Astronomy
&
Astrophysics

On the evolutionary status of Be stars[*,**]

I. Field Be stars near the Sun

J. Zorec[1], Y. Frémat[2], and L. Cidale[3,4,***]

[1] Institut d'Astrophysique de Paris, UMR 7095 CNRS-Université Pierre & Marie-Curie, 98bis Bd. Arago, 75014 Paris, France
e-mail: zorec@iap.fr
[2] Royal Observatory of Belgium, 3 Av. Circulaire, 1180 Bruxelles, Belgium
[3] Facultad de Ciencias Astronómicas y Geofísicas, Universidad de La Plata, Paseo del Bosque S/N, 1900 La Plata, Argentina
[4] Instituto de Astrofísica La Plata, CONICET, 1900 La Plata, Argentina

Abstract. A sample of 97 galactic field Be stars were studied by taking into account the effects induced by the fast rotation on their fundamental parameters. All program stars were observed in the BCD spectrophotometric system in order to minimize the perturbations produced by the circumstellar environment on the spectral photospheric signatures. This is one of the first attempts at determining stellar masses and ages by simultaneously using model atmospheres and evolutionary tracks, both calculated for rotating objects. The stellar ages (τ) normalized to the respective inferred time that each rotating star can spend in the main sequence phase (τ_{MS}) reveal a mass-dependent trend. This trend shows that: a) there are Be stars spread over the whole interval $0 \lesssim \tau/\tau_{MS} \lesssim 1$ of the main sequence evolutionary phase; b) the distribution of points in the (τ/τ_{MS}, $M/M_\odot$) diagram indicates that in massive stars ($M \gtrsim 12\,M_\odot$) the Be phenomenon is present at smaller τ/τ_{MS} age ratios than for less massive stars ($M \lesssim 12\,M_\odot$). This distribution can be due to: i) higher mass-loss rates in massive objets, which can act to reduce the surface fast rotation; ii) circulation time scales to transport angular momentum from the core to the surface, which are longer the lower the stellar mass.

Key words. stars: emission-line, Be – stars: evolution – stars: rotation – stars: fundamental parameters (classification, colors, luminosities, masses, radii, temperatures, etc.)

1. Introduction

Correlations between the Balmer line emission width with $V\sin i$ and the statistical tendency of Be-type emission line profiles to be present for low $V\sin i$ values, while Be-shell type prevails at high $V\sin i$, inspired Struve (1931) model of the Be phenomenon. This model underlies the most recent ones. The model also assumes that there is a secularly stable B-type stellar critical rigid rotator (Tassoul 1978), which builds an extended circumstellar envelope (CE) condensed towards the equatorial plane by equatorial ejection of mass. Be stars are considered to be O, B and A spectral type non-supergiant stars that have shown at least once some emission in the Balmer lines (Jaschek et al. 1981). It has long been known that Be stars are fast rotators and that they rotate at least 1.5 to 2 times faster

than B stars without emission (Slettebak 1979; Zorec 2004). From a homogeneous set of $V\sin i$ parameters, although not corrected for effects of fast rotation, Chauville et al. (2001) concluded that Be stars rotate on average at angular velocity rates $\omega = \Omega/\Omega_c \sim 0.8$. Stoeckley (1968) pointed out that the $V\sin i$ parameters can be systematically underestimated if second order effects of fast rotation on absorption lines are neglected. Making allowance in the calculation of rotational line broadening for star distortion and non-uniform surface temperature in latitude (von Zeipel 1924a,b), Stoeckley (1968) concluded that Be stars might actually be critical rotators. Thus, according to this author "...mild prominence activity or other minor disturbances lead to the ejection of matter..." to form the CE. These arguments were taken up by Owocki (2004) and Townsend et al. (2004). In a study by Frémat et al. (2005) of rotational effects on fundamental stellar parameters it is shown, however, that Be stars rotate on average at $\omega \sim 0.9$.

Crampin & Hoyle (1960) suggested that the Be phenomenon occurs during the secondary contraction phase, where the surface rotation velocity has been spun up as a consequence of angular momentum conservation. Raw photometric color indices place Be stars near, or on, the TAMS (terminal-age

---

main sequence) (Schmidt-Kaler 1964; Schild & Romanishin 1976). However, this apparent location in the HR diagram of some Be stars is due in part to the continuum emission excess produced in CE and to the over-luminosity of the central objects carried by the rotationally-induced stellar geometrical deformation and the concomitant gravitational darkening effect (von Zeipel 1924a,b; Slettebak et al. 1980; Mermilliod 1982; Slettebak 1985; Collins & Sonneborn 1977; Collins et al. 1991; Townsend et al. 2004; Frémat et al. 2005).

If the Be phenomenon is an outgrowth of nearly critical stellar rotation, one of the fundamental questions becomes whether such a fast surface rotation is an innate property, or it is acquired at some stellar evolutionary phase. Two different phenomenological frames were put forward to tackle this question, which depend on whether Be stars are considered binaries or single stars. In binaries the Be phenomenon could arise after a Roche-lobe overflow event, when one of the components gains mass and angular momentum (Packet 1981; Harmanec 1987; Gies 2000). While this mechanism cannot entirely account for the observed frequency of Be stars (Pols et al. 1991; van Bever & Vanbeveren 1997), it can explain Be/X-ray binaries (Coe 2000). Therefore, let us assume that Be phenomenon concenrs only single stars only. In that case, the near critical equatorial velocity can either be an attribute of stars since their ZAMS (zero-age main sequence) phase, or a property that is acquired during their long-lived main sequence (MS) evolutionary phase. Using moments of inertia of non-rotating stellar models, Hardorp & Strittmatter (1970) concluded that the initial rotation at ZAMS must be from 1 to 4% below the critical rate, for the star to become a critical rotator from core contraction in the MS. Since the fast rotation reduces considerably the stellar momentum of inertia, according to Endal (1982) only 40% under-critical rotation at the ZAMS would be needed to accelerate the star to the critical rotation during the MS life span. For the star can reach critical rotation during the MS phase on the stellar surface also depends on the initial amount and internal distribution of angular momentum and on its loss and further redistribution mechanisms (Endal & Sofia 1979; Meynet & Maeder 2000; Heger & Langer 2000; Meynet & Maeder 2002; Maeder & Meynet 2001, 2003; Stępień 2002).

Apart from the mentioned photometric results, few studies deal with the evolutionary status of Be stars. Jaschek et al. (1980) and Hubert-Delplace et al. (1982) noticed a mild tendency of late Be type stars to belong to the giant luminosity class, while early Be type stars have a tendency to be dwarfs as if there was a mass-age selection that underlies the Be phenomenon. Zorec & Briot (1997) found that the frequency of galactic Be stars against spectral type does not differ strongly from one luminosity class to another, which might suggest that the Be phenomenon can appear at any evolutionary stage during the MS phase. In a study of Be stars in open clusters, Feinstein (1990) noticed an increase of the frequency of these objects near the middle of the MS phase. Similarly, Fabregat & Torrejón (2000) concluded that the change of the frequency distribution of Be stars against the spectral type as a function of cluster age could be accounted for by assuming that the Be phenomenon occurs in the second half of the MS phase.

While in the stellar count of field Be stars by Zorec & Briot (1997) the effects from CE-dependent over-luminosity and spectral changes due to fast rotation were taken into account, the binning of stars by luminosity class groups, which was meant to represent an evolutionary-dependent separation, cannot be justified entirely for many stars of the sample. On the other hand, in Feinstein (1990) and Fabregat & Torrejón (2000), the sampling of Be stars in clusters against spectral type can be incomplete. In these environments, Be stars are frequently detected photometrically. Since massive Be stars are scarce and the emission in the Balmer lines of stars cooler than B7 can be low, information on the appearance of the Be phenomenon in the relevant stellar masses may then be missing. Moreover, photometric and spectroscopic spectral types were not corrected for alterations due to the CE nor for changes induced by fast rotation. Thus, due to these shortcomings the conclusions drawn in those attempts are likely biased.

Another way to undestand the evolutionary status of Be stars that may in principle solve the above inconveniences, is to study in detail a statistically significant number of individual Be stars, where in each star the perturbations produced by the circumstellar emission/absorptions on the observed spectra are considered and account is taken of the rotationally-induced effects. The aim of the present paper is thus to discuss the evolutionary stage of a well-observed sample of bright, field galactic Be stars, whose observational data were treated for all these deviations. The fact that these objects are bright enough implies that their Be character is well recorded. This is of particular interest for those objects either among the more or the less massive stars of the sample, because in general they are not so numerous in either of these extremes of mass.

2. Observational data

One of the main concerns related to the analysis of the observational data of Be stars is to remove circumstellar emission/absorption perturbations. We determine the fundamental parameters of these stars using BCD spectrophotometric data (Chalonge & Divan 1952). In this system the Balmer discontinuity is observed, which is characterized by two independent measurable quantities: the flux jump at $\lambda = 3700$ Å, D in dex and the mean spectral position of the discontinuity, λ_1, presented in $\lambda_1 - 3700$ Å. The (λ_1, D) parameters are strong functions of $T_{\rm eff}$ and $\log g$ (Divan & Zorec 1982; Zorec 1986). It has been shown several times that for Be stars these two quantities are free of circumstellar extinction and circumstellar emission/absorption (Zorec & Briot 1991). Be stars may show a Balmer discontinuity with two separated components. While the variable component due to the CE can be, in a given star, either in emission or in absorption depending on the time they are observed (Moujtahid et al. 1998, 1999), the constant component reflects the average photospheric properties of the observed stellar hemisphere (Zorec et al. 2002).

The program stars are listed in Table 1. They were observed for more than 50 years at OHP (France) and ESO (La Silla, Chile) with the Chalonge spectrograph (Baillet et al. 1973), a device specially conceived to observe the stellar Balmer discontinuity. Since 1990 some of the program objects in the

south hemisphere have been observed in CASLEO (San Juan, Argentina) with the Boller & Chivens Cassegrain spectrograph, whose resolution in the low dispersion mode is similar to that of the Chalonge spectrograph (Cidale et al. 2000, 2001) and enables one to separate clearly the stellar from the circumstellar Balmer discontinuity. The (λ_1, D) parameters of the observed stars are listed in Table 1 (Cols. 2 and 3). Their rms deviations are on average $\sigma_D \lesssim 0.005$ dex and $\sigma_{\lambda_1} \lesssim 0.3$ Å.

The (λ_1, D) were calibrated in the $(T_{\text{eff}}, \log g)$ parameters (Divan & Zorec 1982; Zorec 1986). When these calibrations are used for fast rotating stars, they must be considered to represent the aspect angle-averaged properties of the stellar photosphere in the observed stellar hemisphere. Hereafter we call them *apparent* fundamental parameters. The *apparent* $(T_{\text{eff}}, \log g)$ sets are listed in Table 1: T_{eff} and $\log g$ (Cols. 4 and 5). The $V \sin i$ parameters employed in the present work (Col. 6) are from Chauville et al. (2001) and Frémat et al. (2005). The listed $V \sin i$ parameters were obtained using classical models of stellar atmospheres (Stoeckley & Mihalas 1973), where the variation of the limb-darkening coefficient with frequency in the line is taken into account, so that they can be considered free of underestimations induced by the use of constant limb-darkening coefficients (Collins & Truax 1995). Nevertheless, these $V \sin i$ parameters must also be considered *apparent*.

Figure 1 shows the HD diagram of the observed Be stars given in terms of the observed BCD (λ_1, D) parameters. In this diagram we can see the tendency mentioned by Jaschek et al. (1980) and Hubert-Delplace et al. (1982) of late type Be stars (cooler than B5) to be on average slightly more luminous than early Be stars. Although the (λ_1, D) parameters of stars presented in Fig. 1 can be considered free of CE perturbations, they are "apparent" quantities because they still need to be treated for effects induced by fast rotation. Our stellar sample has a spectral type distribution that mirrors quite well that of the whole known Be star population near the Sun (Zorec & Briot 1997). The results we obtain with them can then be considered to represent fairly well the properties of this entire population.

3. Method

3.1. Stellar atmosphere models of rotating stars

The models of rapidly rotating stars used in the present work to describe the aspect angle average spectroscopic and spectrophotometric characteristics of early type stars are described in Frémat et al. (2005) (calculation code FASTROT). They correspond to objects with overall rigid rotation and take into account their geometrical deformation as described by equipotentials in the Roche approximation. Allowance is also made for changes of the polar radius and the bolometric luminosity produced in the stellar core. The lowering of the bolometric luminosity was considered to be related to the mass-compensation effect of rigidly rotating stellar cores (Sackmann 1970; Clement 1979). The non-uniform effective temperature distribution with latitude follows the von Zeipel (1924a,b) theorem as far as high enough temperatures are concerned. For local effective temperatures lower than 8000 K we used the
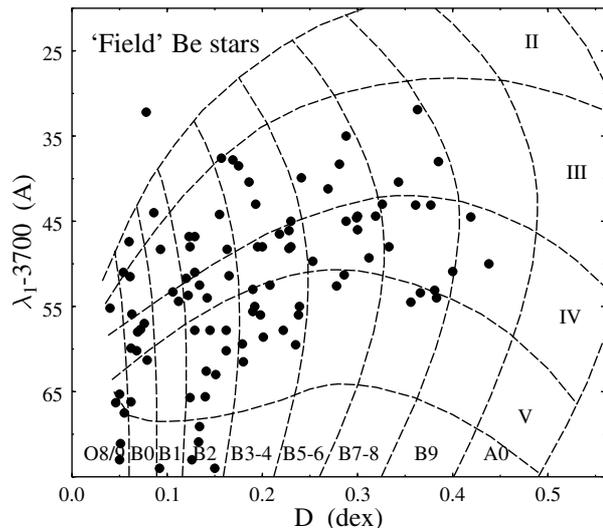

Fig. 1. HR diagram of the program Be stars in terms of the BCD (λ_1, D) parameters. Each curvilinear quadrilateral represents a MK spectral type-luminosity class group. The vertical strips demarcate the spectral types, which are given in the abscissa. The luminosity classes corresponding to the horizontal strips are marked in the quadrilaterals on the right side of the diagram.

gravitational darkening calculated by Claret (1998). The calculation code FASTROT enables us to calculate spectral lines and energy distributions. We can then estimate the changes produced by rotation on the Balmer discontinuity and the (λ_1, D) parameters that describe it.

3.2. Relation between "apparent" and "parent non-rotating counterpart" stellar parameters

The main purpose of the present paper is to infer stellar fundamental parameters that may give us some insight into the most plausible evolutionary state of the studied Be stars, once the observed quantities are treated for the first order rotational effects. To derive the actual stellar mass M of a fast rotator, we assume that the observed set of parameters $(\lambda_1, D, V \sin i)$ is affected by two types of rotational effects. There are direct changes related to the stellar geometrical deformation and the consequent non-uniform surface temperature and gravity distributions. Moreover, there are effects related to changes that the rotation produces on the evolution of stars. In order to take both types of effects into account, we proceed in two steps. Our models are built as a function of effective temperature and surface gravity of homologous spherical stars: the same mass, but without rotation. So, in a first step, from the observed (λ_1, D) quantities we derive the "*parent non-rotating counterparts*" (*pnrc*). In a second step, we use the *pnrc* $(T_{\text{eff}}, \log g)$ sets to derive the $(\overline{T_{\text{eff}}}, \log \overline{g})$ quantities, which are the effective temperature and gravity *averaged* over the whole rotationally-deformed stellar surface. These average quantities are finally used as the entry parameters to the models of stellar evolution with rotation to infer masses and ages. For consistency with other works based on the use of FASTROT, the nomenclature of fundamental parameters follows that adopted in Frémat et al. (2005).

The transition from *apparent* to *pnrc* parameters is carried out considering the following transformations:

$$\left. \begin{array}{rcl} D &=& D_{\mathrm{o}}(T_{\mathrm{eff}}, \log g) \times F_D(T_{\mathrm{eff}}, \log g, \omega, i) \\ \lambda_1 &=& \lambda_1^{\mathrm{o}}(T_{\mathrm{eff}}, \log g) \times F_{\lambda_1}(T_{\mathrm{eff}}, \log g, \omega, i) \\ V \sin i &=& V_{\mathrm{c}}(T_{\mathrm{eff}}, \log g) \times \frac{R_{\mathrm{e}}(T_{\mathrm{eff}}, \log g, \omega)}{R_{\mathrm{c}}(T_{\mathrm{eff}}, \log g)} \omega \sin i \end{array} \right\}, \quad (1)$$

where D and λ_1 are the observed BCD quantities, while D_{o} and λ_1^{o} are those of the rotationless homologous star; T_{eff} and $\log g$ are the *pnrc* fundamental parameters; i is the stellar aspect angle; V_{c} is the critical linear equatorial velocity for rigid rotation; R_{c} is the critical equatorial radius and R_{e} the "actual" equatorial radius at the rotational rate $\omega = \Omega/\Omega_{\mathrm{c}}$. The factors F_D and F_{λ_1} are functions calculated with FASTROT for rigid rotators, which accounts for the geometrical deformation of stars, as well as for the corresponding aspect angle dependent external non-uniform temperature and gravity distributions. Some examples of the behavior of D and λ_1 as a function of the angular velocity rate $\omega = \Omega/\Omega_{\mathrm{c}}$ and inclination angle i for several *pnrc* ($T_{\mathrm{eff}}, \log g$) pairs are shown in Fig. 2.

As in previous calculations of rotational effects on observational quantities of B stars (Maeder & Peytremann 1970, 1972; Collins & Sonneborn 1977; Collins et al. 1991; Townsend et al. 2004; Frémat et al. 2005), the calculations of (λ_1, D) also show that rotational effects become conspicuous at rates $\omega \gtrsim 0.5$. This limit is however lower for lower effective temperature. The (λ_1, D) parameters are double valued functions against ω at low enough *pnrc* effective temperatures ($T_{\mathrm{eff}} \lesssim 13\,000$ K). This occurs as a consequence of the gravitational darkening effect, which changes the average ionization balance in the stellar surface. As in stars with spectral types cooler than A1, the H$^-$ absorption increases progressively over that of b–f transitions of neutral hydrogen, which carries a decrease of the value of D. Similarly, the λ_1 folding at high ω rates reflects the same behavior as in late B-type giant stars, in the sense that pressure broadening effects on Balmer lines makes λ_1 decrease more rapidly the lower the effective temperature as $\log g$ decreases.

Since model evolutionary tracks are presented in terms of fundamental parameters *averaged* over the whole stellar surface ($\overline{T_{\mathrm{eff}}}, \log \overline{g}$), a relation between these quantities and the *pnrc* ($T_{\mathrm{eff}}, \log g$) determined from (1) has to be used to infer stellar masses and ages. Nevertheless, instead of using direct $\overline{X_i} = F(X_{i,j}, \omega)$ relations between *pnrc* and *averaged* X-quantities, we prefer to iterate relations like:

$$\left. \begin{array}{rcl} \overline{T_{\mathrm{eff}}} &=& T_{\mathrm{eff}} \times F_T(M, \tau, \omega) \\ \log \overline{g} &=& \log g \times F_G(M, \tau, \omega) \end{array} \right\} \quad (2)$$

which are essentially of geometrical nature and where the dependency on the stellar age τ and mass M is small. Figure 3 shows the functions F_T and F_G for $M = 3$ and $20\ M_\odot$ at $\tau/\tau_{\mathrm{MS}} = 0.5$.

The $V \sin i$ parameter on the left-hand-side of the third relation in (1) is intended to represent the *true* rotational parameter, i.e. the parameter corrected for underestimations induced by the gravity darkening (Stoeckley 1968; Townsend et al. 2004; Frémat et al. 2005). Since this correction depends on the *pnrc* ($T_{\mathrm{eff}}, \log g$) and ω, it has to be iterated simultaneously as we search for the solution of the system (1).
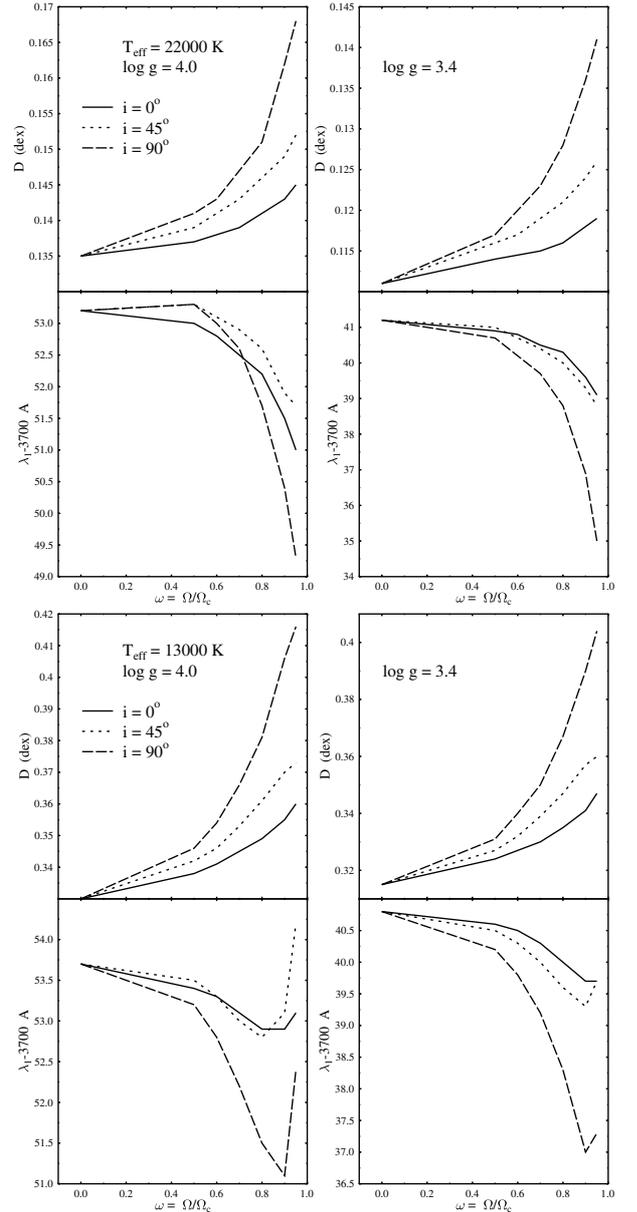

Fig. 2. Model (λ_1, D) parameters against the rate $\Omega/\Omega_{\mathrm{c}}$ for different unperturbed pairs ($T_{\mathrm{eff}}, \log g$) and several aspect angles i.

To solve relations (1) and (2) we need to specify either the angular velocity rate ω or the inclination i. Since it was shown by Frémat et al. (2005) that most Be stars rotate at $\omega = 0.88^{+0.06}_{-0.04}$, which is a distribution with a very low dispersion of angular velocities, we can adopt $\omega = 0.88$ to solve the relations in the sought parameters M, τ and i. In this paper we focus our discussion only on τ and M. We also note that the solution of (1) and (2) implies that we can translate (λ_1, D) into ($T_{\mathrm{eff}}, \log g$). As empirical calibrations cannot be used, because of mixed rotational effects, we use model calculations. This implies that we do not have errors arising from the procedure of translating (λ_1, D) into ($T_{\mathrm{eff}}, \log g$), but only with those passed from the observed BCD quantities onto the *apparent* fundamental parameters. The propagation of empirical uncertainties in the determination of (τ, M) is discussed in Sect. 4.2.
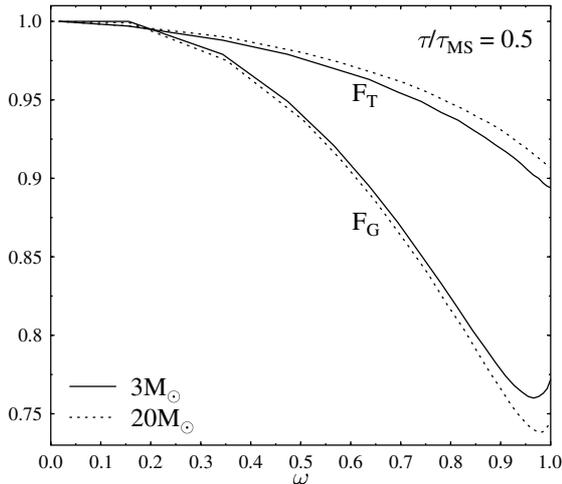
Fig. 3. Functions F_T and F_G for $\tau/\tau_{MS} = 0.5$ and two stellar masses.

3.3. Evolutionary tracks of rotating stars

Model tracks of stellar evolution with rotation calculated by Meynet & Maeder (2000, MM2000) for solar chemical composition $Z = 0.02$ were done for different initial (or ZAMS) true equatorial rotation velocities V_o. In these models it is also assumed that in the ZAMS the stars start evolving as rigid rotators. The use of evolutionary tracks with rotation has two difficulties:

a) no information exists on what V_o should be adopted to interpolate stellar masses and ages. Zorec et al. (2004) have shown that the true equatorial velocities of dwarf Be stars have a quite flat distribution against spectral type around $V \simeq 300$ km s^{-1} ($\overline{V} \simeq 350$ km s^{-1} at BV0 and $\overline{V} \simeq 270$ km s^{-1} for BV9). Calculations of internal angular momentum redistribution foresees that in the first 1 to 2% of the MS lifetime an initial flat internal angular velocity distribution transforms into a step-like one, where, depending on the mass, the rotation in the stellar core becomes 20% to 40% faster than in the envelope (Denissenkov et al. 1999; Meynet & Maeder 2000). Since classical Be stars have masses that range from 3 to 30 $M_\odot$, we should then use models of stellar evolution calculated for somewhat higher mass-dependent initial velocities, ranging from $V_o \simeq 340$ at 3 $M_\odot$ to 420 km s^{-1} for 30 $M_\odot$;

b) there is some evidence for internal angular momentum redistribution in the pre-main-sequence (PMS) evolutionary stages of stars with masses from 0.1 to 10 $M_\odot$ (Wolff et al. 2004) which implies that stars can start evolving from the ZAMS as differential rotators. If so, and depending on the PMS evolutionary characteristics of individual stars, the amount of rotational energy stored by them could be higher than the limit imposed by the critical rigid rotation (Tassoul 1978). In such a case there is a much higher mass-compensation effect on the core bolometric luminosity and there may be more consequences on the stellar evolution than those accounted for in models used in the present work.

Facing the quoted unknowns on the internal rotation of the studied stars at the ZAMS and on their initial equatorial velocity, we estimate the effect on the mass and age estimates in

the physical framework defined by the existing calculations of stellar evolution with rotation.

First, we obtained stellar ages and masses with the evolutionary tracks without rotation for $Z = 0.02$ (Schaller et al. 1992). Then, we derived the same quantities using the evolutionary tracks for $V_o = 300$ km s^{-1} and $Z = 0.02$ of MM2000. These last correspond to initial angular velocity rates that range from $\omega_o = 0.79$ at $M = 3\ M_\odot$ to $\omega_o = 0.52$ for $M = 30\ M_\odot$. They produce smaller effects on the mass and age estimates than the slightly higher velocities $V_o = f(M)$ needed to produce the average main sequence $V \simeq 300$ km s^{-1} after having undergone rapid initial internal angular redistribution in the ZAMS. The enhanced values $V_o = f(M)$ imply rotational effects on stellar evolution scaled in terms of initial rates ranging from $\omega_o = 0.87$ at $M = 3\ M_\odot$ to 0.70 for 30 $M_\odot$. This difference in the initial rates ω_o may have some significance, since rotationally-induced effects on the stellar fundamental parameters increase rapidly once $\omega > 0.8$ and they are stronger for lower stellar mass (Frémat et al. 2005).

In order to estimate an order of magnitude of the effects on the estimates of mass and age by initial equatorial velocities larger than those used in the published models, we re-scaled the existing evolutionary tracks as a function of the abovementioned mass-dependent values $V_o = f(M)$.

3.4. Re-scaled evolutionary tracks

The calculations carried out by Endal & Sofia (1979) and more recently by Heger & Langer (2000); Meynet & Maeder (2000, 2002) and Maeder & Meynet (2001) show that rotation introduces several changes in the evolutionary tracks compared to those for non-rotating stars. The characteristics of these changes, under the assumption that the stars start evolving from the ZAMS as rigid rotators, depend on: the adopted mass-loss rates, the initial conditions such as chemical composition and the initial rotational velocity V_o and on the mechanisms of angular momentum redistribution inside the star. In Be stars, the average mass-loss rate $\lesssim 10^{-9}\ M_\odot$ yr^{-1}, which encompasses winds and discrete mass ejections, cannot lead to sensitive deviations from the evolution with the time-dependent variation of stellar mass already foreseen in the existing calculations. In this work, those changes of mass are assumed to be the same as that calculated for objects evolving with $V_o = 300$ km s^{-1}. However, depending on the initial value of the rotational velocity and the further phenomenon of angular momentum redistribution, there are at least three other outstanding changes in the evolutionary tracks of rotating stars in the MS phase that interest our fundamental parameter determination:

i) In the $(\log L/L_\odot, T_{\text{eff}})$-plane the tracks are slightly shifted and rotated, so that for a given mass the starting point in the ZAMS is located at a lower temperature and luminosity, which reveals the rotationally-induced mass-compensation effect (Sackmann 1970);

ii) The MS phase is prolonged to higher luminosities than in the non-rotation models due to the enlargement of the H-content in the convective core, which is produced by the mixing processes that fuel it with fresh hydrogen

(Heger & Langer 2000; Meynet & Maeder 2000). On the other hand, as evolution proceeds in the MS phase, in rotating stars there is a more sensitive change of the moment of inertia than in non-rotating objects (Endal 1982; Meynet & Maeder 2000), which leads to an enhanced stretching of the star. The MS phase can then end up at lower surface-averaged effective temperatures than in non-rotating models;

iii) The overall evolutionary MS life span outlasts the non-rotating case, on the one hand because the levitation effect produced by the rotation makes stars behave as is they had a lower effective mass (Sackmann 1970; Bodenheimer 1971; Clement 1979; Moss & Smith 1982) and on the other hand, because the mixing processes cited in *ii*) increase the core-burning lifetime (Heger & Langer 2000; Meynet & Maeder 2000).

These effects give a first order insight into the changes induced by the rotation, which actually encompass a series of subtle global and local mechanisms of mixing and angular momentum redistribution, whose incidence on the stellar structure can be appreciated only through detailed calculations. In this work we use the final settings of such calculations carried out by MM2000 to re-scale the evolutionary tracks for initial velocities V_o at will. We use the term "re-scale" instead of "interpolate", because some effects calculated in detail have been published explicitly only for a restricted number of stellar masses and sometimes they were typified by a single case that we had to generalize. Only the MS phase was treated in this way. The ($\log L/L_\odot$, $\log T_{eff}$) evolutionary paths in the post-MS part were constructed by translating the predictions given by model-evolution without rotation. Since by definition Be stars are non-supergiant, the supergiant region will rarely be used in the present work. The results of this re-scaling operation is shown in Fig. 4. We see there: 1) evolutionary tracks for non-rotating stars (dotted lines); 2) model tracks by MM2000 calculated with $V_o = 300$ km s^{-1} in all masses (full lines); 3) re-scaled tracks for a linear enhancement of the initial velocity V_o above 300 km s^{-1} as a function of mass given by $V_o = 300 + [3 \times (M/M_\odot) + 30]$ km s^{-1} (dashed lines). This relation is intended to give the initial velocities so that after the first $\approx 10^4$ yr in the MS phase the Be star true equatorial velocities become $V \simeq 300$ km s^{-1} as observed (cf. Sect. 3.3).

Changes of initial velocities from $V_o = 300$ km s^{-1} to $V_o = 300 + [3 \times (M/M_\odot) + 30]$ km s^{-1} seem not to produce huge effects on the evolution path shapes. This saturation effect noted for high V_o values was already commented on by MM2000 for hot rotating stars, where increased mass-loss rates due to a faster rotation partially suppress the effects related to an enhanced outward transport of angular momentum. Our "transcription" of the phenomenon in all masses for whatever V_o may perhaps be insufficient as it depends on a simple interpolation among the few cases given explicitly in the literature (Talon et al. 1997; Meynet & Maeder 2000). However, we note in Fig. 4 that: 1) the breadth of the MS phase of rotating models is slightly enlarged for all OB stellar masses as compared to the rotationless case; 2) the stellar mass that corresponds to a given ($\log L/L_\odot$, $\log T_{eff}$) point inferred in the lower half of the MS phase of rotating objects will be slightly higher than the same obtained with tracks of non-rotating models; 3) stellar masses inferred in the upper half of the MS will
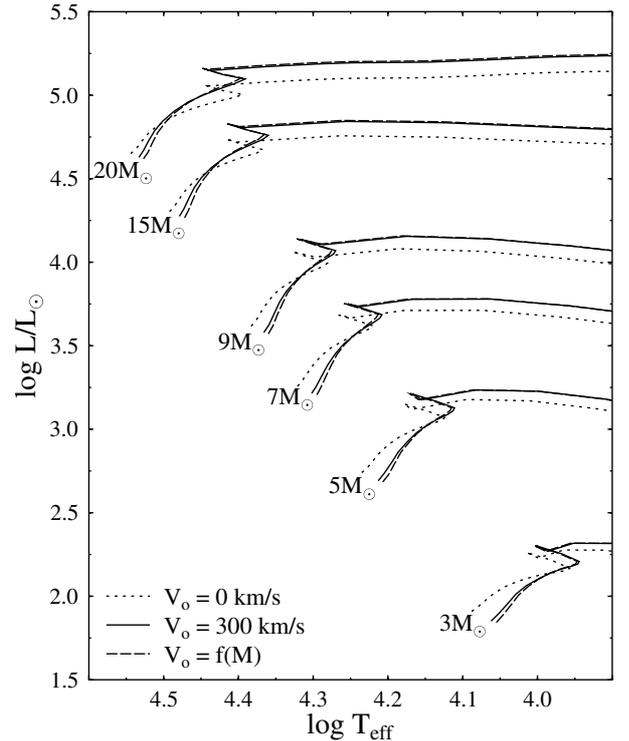

Fig. 4. Evolutionary tracks for different initial velocities V_o. "*dotted*" lines are for evolutionary tracks with $V_o = 0$ km s^{-1}; "*full*" lines are for $V_o = 300$ km s^{-1}; "*dashed*" lines correspond to $V_o = f(M)$ so that $V_o = 340$ km s^{-1} at 3 $M_\odot$ and 420 km s^{-1} for 30 $M_\odot$.

not depend sensitively on the type of evolution model used, if masses are lower than $\sim 10 \, M_\odot$, while for stars with $M \gtrsim 10 \, M_\odot$ the masses obtained from rotation-dependent tracks will be lower compared to those interpolated with rotationless evolutionary paths.

3.5. Stellar ages

The evolution time scales depend on the total angular momentum and its progressive internal redistribution. Let us call τ_{MS}^o the time spent in the MS phase by a non-rotating star (from ZAMS to TAMS) and use the notation τ_{MS} for the MS life span of its homologous rotating object. Assuming that stars have rigid rotation in the ZAMS, so that their initial equatorial velocity is V_o, MM2000 have shown that between τ_{MS} and τ_{MS}^o the following relation holds:

$$\frac{\tau_{MS}}{\tau_{MS}^o} = 1.0 + \alpha \overline{V_{MS}}(M, V_o) \tag{3}$$

where $\alpha = 0.0013$ and $\overline{V_{MS}}(M, V_o)$ in km s^{-1} is the surface rotational velocity averaged over the whole τ_{MS} period. On account of the simplicity of relation (3) and that actually we do not have another way to scale stellar ages on evolutionary tracks for whatever initial values of V_o, under the assumption that stars are rigid rotators in the ZAMS, let us write a similar relation to (3) for the age $\tau(\omega)$ of a rotating object at any

Table 2. Ratios γ as a function of mass and the initial angular velocity rate $\omega_o = f(V_o/V_c)$.

$M/M_\odot$	$\omega_o = 0.5$	0.8	0.9
20.0	-0.022	-0.008	-0.008
15.0	-0.011	0.021	0.029
10.0	0.003	0.056	0.074
5.0	0.022	0.113	0.154
3.0	0.036	0.170	0.242

moment of its MS evolutionary phase and the respective "rest" age $\tau^o = \tau(\omega = 0)$:

$$\frac{\tau(\omega)}{\tau^o} = 1.0 + \frac{\alpha}{\tau(\omega)} \int_0^{\tau(\omega)} V(t)\mathrm{d}t \qquad (4)$$

where $V(t)$ is the time dependent surface velocity. After a rapid decrease that lasts 1 to 2% of the MS lifetime, in massive stars with mass-loss, $V(t)$ shows a roughly "linear" decrease with time (MM2000), while in stars with masses $M < 10\,M_\odot$, where mass-loss is negligible, it follows a "parabolic" increase (Endal 1982; Meynet & Maeder 2000). We can then derive the following relation between the age fraction spent in the MS phase by a rotating star and the homologous non-rotating object:

$$\frac{\tau(\omega)}{\tau_{\mathrm{MS}}} = \frac{(\tau^o/\tau^o_{\mathrm{MS}})}{1 + \gamma(\tau^o/\tau^o_{\mathrm{MS}})} \qquad (5)$$

in which we have:

$$\gamma \simeq \left[\frac{\overline{V_{\mathrm{MS}}}(M, V_o)}{V_o} - q(M, V_o) \right] \left(\frac{\alpha V_o}{1 + q(M, V_o)\alpha V_o} \right) \qquad (6)$$

where $q(M, V_o) = V_i/V_o < 1$; V_i represents the surface equatorial velocity after the very initial short-lasting internal angular momentum redistribution. Using the values of V_i/V_o and $\overline{V_{\mathrm{MS}}}(M, V_o)$ as a function of M and V_o from MM2000 and Denissenkov et al. (1999) we obtained the estimates of γ that are given in Table 2. We see there that in many cases it is $|\gamma| < 0.1$ so that to a good approximation:

$$\tau(\omega) \simeq \tau_{\mathrm{MS}} \left(\frac{\tau^o}{\tau^o_{\mathrm{MS}}} \right). \qquad (7)$$

On the other hand, the small values of $|\gamma|$ warrant that a very detailed representation of the function $V(t)$ is not relevant to evaluate the age ratios (5).

Since we will be dealing with $\omega \gtrsim 0.8$, most Be stars studied will have $\tau(\omega)/\tau_{\mathrm{MS}} \lesssim \tau^o/\tau^o_{\mathrm{MS}}$. In general deviations from (7) are small and, as expected, they are higher the lower the mass.

For interpolation of stellar ages, we divided the ZAMS-TAMS time interval of each evolutionary path into 100 parts: τ_i, $i = 0,1,...100$, so that $\tau_0 = \tau_{\mathrm{ZAMS}}$ and $\tau_{100} = \tau_{\mathrm{TAMS}} = \tau_{\mathrm{MS}}$. Times τ_i for the same i in tracks of two consecutive masses were considered representing stars in homologous evolutionary stages. Interpolations of masses and ages were then done in the $(\log L, \log T_{\mathrm{eff}})$ diagrams according to this criterion of homologous evolution.

A few studied objects fall in the HR-diagram strip of the secondary contraction phase. This does not allow us to decide if these objects are still in the MS phase, in the secondary contraction region, or of they are already in the giant branch. We treated them as if they still were in the MS, since the short time scales involved in the remaining phases do not change much the estimate of the age ratios τ/τ_{MS}. A small number of stars remain in the post-MS phase, even after all corrections of parameters for rotational effects. In the giant phase the evolution times were re-scaled using a relation similar to (7).

4. Results

4.1. Preliminaries

The major motivation of the present paper is to infer the "present-day" age of stars already displaying the Be phenomenon. We cannot say if the phenomenon has already been present in a given star for some time, or if the star will display it up to the end of its MS phase.

As alredy noted, Frémat et al. (2005) have shown that most Be stars rotate at $\omega \simeq 0.88$. Since this rate applies to stars that can be at different evolutionary stages in the MS phase, only those tracks that imply a state of the surface velocity that fit the condition $\omega \simeq 0.9$ at the required location of the star in the HR-diagram would be suitable to infer its mass and age. However, we do not know the individual initial velocities V_o to build the required model tracks. This can be solved partially by iterating the stellar mass and its V_o. Nonetheless, the operation requires a number of subtleties that are beyond the scope of the present work and will be developed elsewhere. The results obtained in this section will show a posteriori that adopting an appropriate V_o for all stars is an approximation that suffices for the purposes of the present work. So, in the present paper we calculate masses and ages adopting the models by MM2000 for $V_o = 300$ km s^{-1}. We estimate the magnitude of possible uncertainties caused by the lack of knowledge of the specific value of V_o. To this end, we determine the $(\tau/\tau_{\mathrm{MS}}, M/M_\odot)$ parameters of several HR "test" points in the upper and lower half of the MS phase (chosen at hoc), as a function of evolutionary tracks dependent on different values of V_o. We assume that the "test" points correspond to stars rotating at $\omega = 0.88$. A given set of test *apparent* parameters produce, as expected, inclination angle-dependent series of *pnrc* and *averaged* fundamental parameters. However, the relative changes from the use of various evolutionary tracks are the same. So, we assume that the test objects are seen at $i \simeq 52^o$, or an average inclination of rotation axes oriented at random ($52^o \simeq \arcsin[\overline{\sin i} = \pi/4]$). For this specific angle, *apparent* $X(i)$ fundamental parameters and the respective surface *averaged* $\overline{X}$ obey: $X(i \simeq 52^o) \sim \overline{X}$ (the Xs stand for $\log L$, $\log g$, $\log T_{\mathrm{eff}}$, etc.).

The results thus obtained are displayed in Table 3. The $(T_{\mathrm{eff}}, \log g)$ parameters given in Cols. 1 and 2 of the 1st block in Table 3 represent the observed, i.e. *apparent*, fundamental parameters which need to be treated for rotational effects. In Cols. 3 to 5 of the 1st block are given the masses, ages and fractions of age spent in the MS as reflected by models of stellar evolution without rotation (Schaller et al. 1992).

Table 3. Comparison of masses, ages and age ratios derived from evolutionary tracks without and with rotation.

Nᵒ	$T_{\rm eff}$	$\log g$	$M/M_\odot$	τ (age)	$\tau/\tau_{\rm MS}$
	K	dex		years	
1	Apparent parameters		Evolution without rotation		
	36 324	4.043	24.78	2.24×10^6	0.350
	29 119	3.449	24.03	5.70×10^6	0.900
	27 102	4.100	11.98	5.53×10^6	0.350
	23 529	3.630	11.93	1.41×10^7	0.900
	14 302	4.157	4.00	5.72×10^7	0.350
	12 169	3.695	4.00	1.46×10^8	0.900
2	*pnrc* parameters for		Evolution without rotation		
	$\Omega/\Omega_{\rm c} = 0.88$				
	38 903	4.185	27.67	2.68×10^5	0.046
	30 941	3.563	25.10	5.16×10^6	0.841
	29 169	4.234	13.15	4.23×10^5	0.031
	25 291	3.751	12.67	1.16×10^7	0.807
	15 484	4.280	4.28	7.37×10^6	0.054
	13 176	3.808	4.19	1.18×10^8	0.818
3	Averaged parameters		Evolution without rotation		
	for $\Omega/\Omega_{\rm c} = 0.88$				
	36 529	4.037	25.35	2.24×10^6	0.359
	29 026	3.437	24.24	5.67×10^6	0.900
	27 077	4.089	12.12	6.29×10^6	0.407
	23 478	3.622	12.15	1.39×10^7	0.910
	14 294	4.149	4.06	6.62×10^7	0.425
	12 163	3.690	4.09	1.41×10^8	0.922
4	Averaged parameters		Evolution with rotation		
	for $\Omega/\Omega_{\rm c} = 0.88$		$V_{\rm o} = 300$ km s^{-1} ∀ masses		
	36 545	4.046	25.88	2.31×10^6	0.299
	28 991	3.411	22.83	7.60×10^6	0.893
	27 089	4.106	12.61	5.08×10^6	0.284
	23 473	3.614	11.92	1.64×10^7	0.863
	14 294	4.171	4.27	4.10×10^7	0.241
	12 163	3.690	4.10	1.59×10^8	0.842
5	Averaged parameters		Evolution with rotation		
	for $\Omega/\Omega_{\rm c} = 0.88$		$V_{\rm o} = f(M) \gtrsim 300$ km s^{-1}		
	36 566	4.058	26.61	2.00×10^6	0.253
	28 989	3.410	22.75	8.02×10^6	0.898
	27 094	4.115	12.85	4.38×10^6	0.243
	23 473	3.614	11.92	1.69×10^7	0.867
	14 294	4.176	4.32	3.44×10^7	0.204
	12 163	3.690	4.10	1.63×10^8	0.846

Nᵒ = block identifier to indicate in the text the type of evolutionary model used.

In Cols. 1 and 2 of the 2nd block are displayed the respective sets of *pnrc* ($T_{\rm eff}$, $\log g$) parameters of test points. They correspond to parameters the stars would have at rest. In Cols. 3 to 4 of the 2nd block we display the "fictitious" quantities if

the *pnrc* fundamental parameters were used to derive masses and ages from evolutionary models without rotation. The *pnrc* parameters ($T_{\rm eff}$, $\log g$) given in Cols. 1 and 2 of the 2nd block were derived using the Frémat et al. (2005) model atmospheres for rotating stars. Since evolutionary tracks of rotating stars are given in terms of fundamental parameters *averaged* over the rotationally-deformed stellar surface, in Cols. 1 and 2 of the 3rd, 4th and 5th blocks we give the surface *averaged* effective temperatures and gravities of the test stars rotating at $\Omega/\Omega_{\rm c} \simeq 0.88$. In Cols. 3 to 5 of the 3rd block are given the masses, ages and fractions of MS ages derived using evolutionary tracks without rotation, while in the same columns of the 4th and 5th blocks we give the parameters inferred using the original models by MM2000 with $V_{\rm o} = 300$ km s^{-1} in the ZAMS and the re-scaled evolutionary tracks for the $V_{\rm o} = f(M)$ meant to account for the average $V = 300$ km s^{-1} of dwarf Be stars after the initial fast redistribution of the internal angular momentum (Sect. 3.3).

The figures in Table 3 reveal that for mass estimates, the uncertainties from possible mismatches between $V_{\rm o}$ and $\Omega/\Omega_{\rm c}$ at the required location of the star in the HR diagram are not higher than 1 $M_\odot$ for $M \gtrsim 10$ $M_\odot$ and they are much smaller for masses $M \lesssim 10$ $M_\odot$. There may be, however, strong differences in the absolute age estimates. These differences have to be taken into account when comparisons must be done with ages of stars in environments like clusters that were inferred from non- or slowly-rotating stars. Fortunately, the age fractions $\tau/\tau_{\rm MS}$ are much less sensitive to detailed calculations of stellar evolution. From the 4th and 5th block we see that the choice of tracks with rotation results in higher uncertainties on the fractions $\tau/\tau_{\rm MS}$ in the first evolutionary stages of the MS phase than the end of this phase.

We can then conclude that mass determinations are not strongly sensitive to the type of evolutionary track used. On the other hand, the use of models for rotating stars that take into account the average rotational charactersitics of fast rotators in the dwarf state of the MS leads to estimates of fractional ages which are not sensitive to the specific initial value of $V_{\rm o}$ around 300 km s^{-1}. This ensures that the models used in the present work lead to reliable statistical insights on global distributions and possible mass-dependencies of fractional ages at which the Be phenomenon occurs. It could be, however, suitable to proceed to more detailed iterations when discussing individual objects whose absolute ages are to be determined.

4.2. Application to observed stars

The entry parameters used to derive stellar masses and ages using relations (1) and (2) were considered with their 1σ uncertainty bars: $X = X_{\rm o} \pm \sigma_x$ ($X_{\rm o}$ stands for surface averaged $\log L$ or $\log g$ and $\log T_{\rm eff}$). Each interval ($X_{\rm o}-\sigma_x$, $X_{\rm o} + \sigma_x$) was divided into 7 parts, so that the solutions of relations (1)−(2) and for each star interpolations in the HR diagrams were performed for all possible combinations of individual sub-X_i entry parameters. Hence, for each star we obtained 8^2 solutions that determined the respectively τ- and M-distributions of the solutions (most of them are not symmetrical). From these
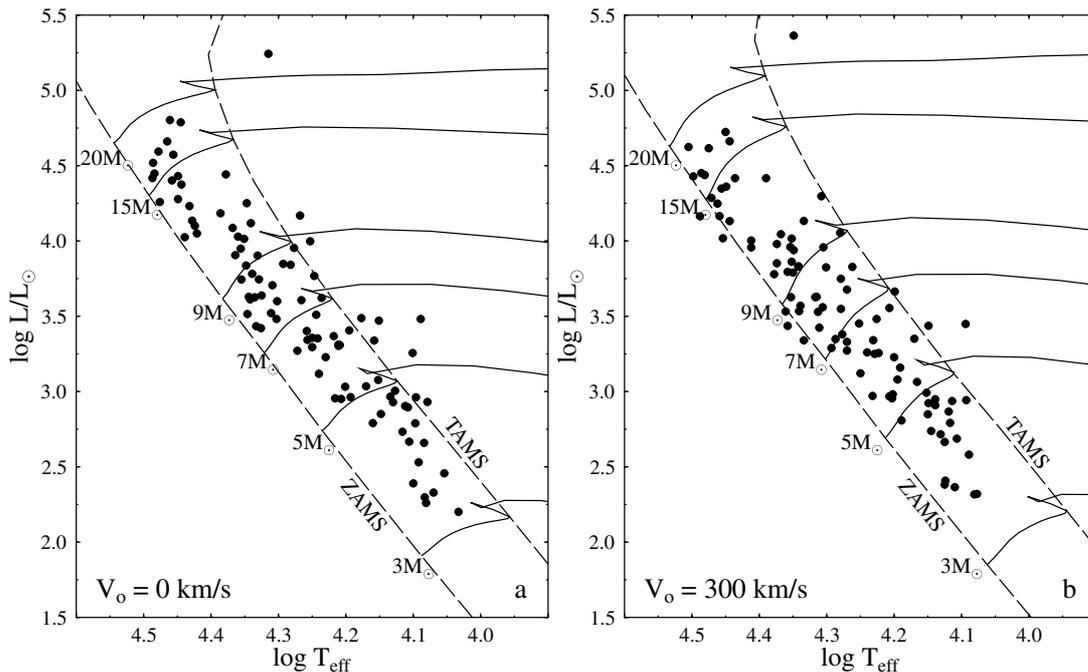
Fig. 5. HR diagrams of the studied Be stars. **a)** Apparent ($\log L/L_\odot$, $\log T_{\mathrm{eff}}$) with evolutionary tracks without rotation. **b)** Surface averaged ($\log L/L_\odot$, $\log T_{\mathrm{eff}}$) and evolutionary tracks with initial an equatorial rotation velocity $V_\mathrm{o} = 300$ km s^{-1} for all masses.

distributions we adopted the *modes* as the most probable results, as well as the corresponding average 1σ dispersion, to account for the related uncertainties. We note that the uncertainties affecting the *apparent* fundamental parameters are those from the observed (λ_1, D) quantities. We also have the uncertainty of $(+0.06, -0.04)$ around the adopted rotation rate $\omega = 0.88$ that could affect the results. Nevertheless, the global changes that will imply on the $(\tau/\tau_{\mathrm{MS}}, M/M_\odot)$ diagram the treatment of the fundamental parameters with $\omega = 0$ or $\omega = 0.88$, justify neglecting the small dispersion $\delta\omega = +0.06, -0.04$. The *apparent* and surface *average* $(T_{\mathrm{eff}}, \log g)$ sets are given in Table 1. In this table we also reproduce the obtained ages, masses and MS age fractions derived using evolutionary models without and with rotation.

Figure 5a shows the HR diagram of the studied stars in terms of their apparent $(\log L, \log T_{\mathrm{eff}})$ parameters and where are shown also the evolutionary tracks for non-rotating stars (Schaller et al. 1992). Figure 5b shows the HR diagram of the same stars, but in terms of their surface *averaged* ($\log \overline{L/L_\odot}$, $\log \overline{T}_{\mathrm{eff}}$) quantities, where we assumed all stars rotate at $\omega = 0.88$. In this figure are also shown the evolutionary tracks for rotating objects that start evolving from the ZAMS as rigid rotators with equatorial velocity $V_\mathrm{o} = 300$ km s^{-1} (MM2000).

In spite of the widened MS phase of rotating stars and corrections made to their fundamental parameters for rotational effects, four program stars lie in the post-MS "bright giant" region. They are HD 23630, HD 45910, HD 183656 and HD 217675, whose true $V\sin i$ in km s^{-1} and estimated inclinations i are (149; 45°), (254; 76°), (274; 77°) and (272; 90°) respectively. These objects are referenced in the literature

as binaries or multiple systems. Their apparently too "evolved" character could be due to a merging effect of fundamental parameters from several components.

The translation of the HR positions in Fig. 5 into masses $M/M_\odot$ and age fractions τ/τ_{MS} is given in Table 1 and in Fig. 6. Figure 6a shows the distribution of points $(\tau/\tau_{\mathrm{MS}}, M/M_\odot)$ obtained for the program stars using the original or *apparent* fundamental parameters and the evolutionary tracks without rotation (Schaller et al. 1992). The plotted error bars correspond to the 1σ dispersions of the $8^2\tau/\tau_{\mathrm{MS}}$- and $M/M_\odot$- solution distributions. Figure 6b shows the same type of distribution, but where parameters were obtained using surface *averaged* fundamental parameters for $\omega = 0.88$ and models of stellar evolution with rotation calculated by MM2000 for $V_\mathrm{o} = 300$ km s^{-1}.

We note that the uncertainty bars affecting the mass determinations are small, while those concerning the MS life fractions are in most cases quite large. This indicates that errors in the determined quantities due to approximate choices of V_o can be concealed within the uncertainties related to the observations.

In both diagrams of Fig. 6, points are spread over the whole interval of age fractions $0.0 \lesssim \tau/\tau_{\mathrm{MS}} \lesssim 1.0$, which suggest that the Be phenomenon may appear at any stage of the stellar evolution in the MS evolution phase. There is, however, a difference between solutions where rotation is taken into account and those where it is not. If we were not aware of rotational effects, Fig. 6a would suggest that 86% of stars are above the $\tau/\tau_{\mathrm{MS}} = 0.5$ limit. Figure 6b shows, however, that when the fast rotation of Be stars is taken into account, the fraction of stars in our sample above $\tau \simeq 0.5\tau_{\mathrm{MS}}$ drops to 62%.
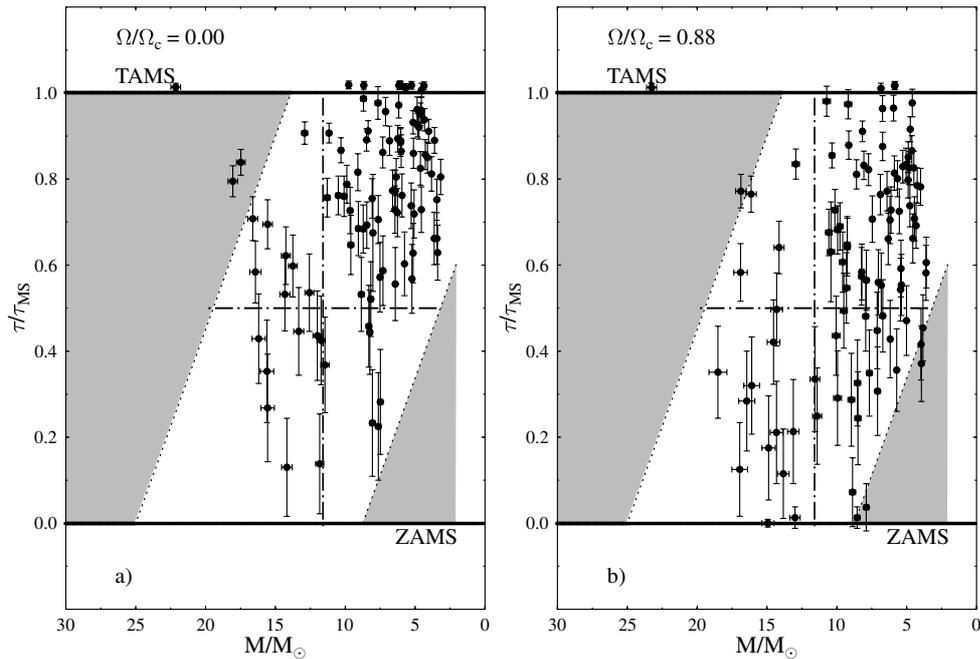
Fig. 6. Age ratios τ/τ_{MS} of the studied Be stars against the mass. **a)** Parameters derived using evolutionary tracks without rotation; **b)** parameters derived using evolutionary tracks with rotation.

Another important result appears when we separate the stars into *massive* ($M \gtrsim 12\ M_\odot$) and *less massive* ones ($M \lesssim 12\ M_\odot$). We see then that in Fig. 6b that the stars are distributed as follows:

	$M \gtrsim 12\ M_\odot$	$M \lesssim 12\ M_\odot$
[upper MS half]	30%	65%
[lower MS half]	70%	35%

The mass-dependent division of Be stars regarding their position with respect to $\tau = 0.5\tau_{MS}$ implies that *the Be phenomenon in massive stars tends to appear on average at smaller τ/τ_{MS} age fractions than in the less massive stars*. The same phenomenon is also suggested in Fig. 6b by the stars with $M \lesssim 12\ M_\odot$ in the lower MS half region, as they all lie above a diagonal that starts among the more massive objects at $\tau/\tau_{MS} = 0$ and ends at $\tau/\tau_{MS} \simeq 0.5$ for $M \simeq 3\ M_\odot$. Since dwarf Be stars rotate on average with $V \simeq 300$ km s^{-1} (Zorec et al. 2004), either we adopted $V_0 = 300$ km s^{-1} or $V_0 = f(M) \gtrsim 300$ km s^{-1}. It can be shown that the initial angular velocity rate ω_0 is higher the lower the stellar mass (cf. Sect. 3.3). The fact that in the $M \lesssim 12\ M_\odot$ region stars are above this well defined mass-dependent slope might suggest that the mechanisms of angular momentum transport that accelerate the stellar surface up to a near/or critical velocity have relatively longer time scales as the stellar masse decreases.

We also obtained masses and age ratios τ/τ_{MS} with the re-scaled evolutionary tracks for $V_0 = f(M) \gtrsim 300$ km s^{-1} (cf. Sect. 3.4). The tilted character of the trend of points obtained is the same as the one presented in Fig. 6b. There is, however, a slightly more pronounced downward drift of points.

In Fig. 6 we notice that 72% of the studied objects have masses from 3 to 12 $M_\odot$. On the other hand, there is a striking lack of massive Be stars with $M \gtrsim 16\ M_\odot$. This lack can be due to several reasons: 1) smaller IMF for massive objects; 2) the fast evolution of massive stars, so that many of them in the solar neighbouring regions could have alreday migrated towards the supergiant phase; 3) the CE can be blown away by the radiation pressure of the "potential" hottest Be stars (Massa 1975).

5. Discussion

5.1. Comparison with previous works

The HR diagram drawn in terms of the *apparent* BCD (λ_1, D) parameters confirms the tendency noticed by Jaschek et al. (1980) and Hubert-Delplace et al. (1982) that late-type Be stars can be on average slightly more luminous than early Be stars. This result can also be likened to the trend shown in Fig. 6a which concerns the apparent stellar parameters.

Our finding of the Be phenomenon appearing at any evolutionary phase is in agreement with similar assertions by Mermilliod (1982) and Slettebak (1985) based on studies of Be stars in clusters. However, the scatter of points over the whole MS life span found by these authors can in part be due to the photometric data that were not corrected for CE perturbing effects and changes introduced by the fast rotation.

Zorec & Briot (1997) have concluded that the frequency of Be stars as a function of spectral type is roughly the same in all luminosity classes. These authors have dealt with a sample of field Be stars three times larger than the sample studied in the present work. However, they have gathered the studied objects in three wide groups of luminosity classes, where both evolutionary and rotational effects on the apparent luminosity

class were mixed. Statistical corrections for CE flux excesses and for changes related to fast rotation were introduced. Since these corrections focused on the countings per group of luminosity class separately, they concerned only absolute magnitudes and spectral types. Moreover, in the number frequencies $N(Be)/N(B+Be)$ against spectral type, not only do B stars without emission greatly outnumber Be stars, but they represent a highly heterogeneous group in physical characteristics. Their evolution then has different characteristics to that of Be stars, which is thus a source of deviations in the count frequencies that cannot be ascribed to Be stars. Hence, the result found by Zorec & Briot (1997) should be considered as intermediate to those shown in Figs. 6a and 6b.

When it comes to Be stars in clusters, statistics can be incomplete in the hotter and in the cooler extremes of spectral types. The scarcity of massive Be stars was already discussed in Sect. 4.2. To this add the possible exclusion of genuine massive Be stars in young clusters. In the accretion pre-main-sequence (PMS) star formation paradigm (Palla & Stahler 1993; Beech & Mitalas 1994), stars with masses $M \gtrsim 10\ M_\odot$ (Behrend & Maeder 2001; Maeder & Behrend 2002) may have a period of MS life when they can still be imbedded in the protostellar nebula. At these early evolutionary stages, there may be genuine fast rotators that have already formed, by mass-loss processes, some circumstellar disc. Thus, their observed emission has two sources, the disc and the leftovers from the accretion nebula. In spite of their mixed Be and Herbig AeBe character, these objects should not then be discarded from the Be statistics. For late type Be stars, their number is reduced because the low effective temperature maintains hydrogen atoms almost neutral, thus disabling possible existing CE to produce observable Balmer emission. Since the existing studies of frequencies of Be stars in clusters have not taken into account rotationally-induced effects in the spectral classifications, they should be compared with our results presented in Fig. 6a. Thus, if in this figure we disregard Be stars with masses $M \gtrsim 12\ M_\odot$ and $M \lesssim 5\ M_\odot$ to mimic possible misdetections, we can see that the stars in the upper half of the diagrams widely outnumber those in the lower half. This readily accounts for the suggestion made by Fabregat & Torrejón (2000) that the Be phenomenon tends to appear in the second half of the MS life time.

5.2. Tilted distribution of points

Let us discuss briefly the tilted trend of points shown in Fig. 6b. It is known that the mass-loss phenomenon in Be stars has two main components: a) winds with rates of the order of $\dot{M} \sim 10^{-9}\ M_\odot\ \mathrm{yr}^{-1}$; b) discrete mass-loss events of $\delta M \sim 10^{-9}\ M_\odot$ underlying light outbursts several times per year (Hubert et al. 2000; Zorec 2004). Be stars with masses $M \lesssim 12\ M_\odot$ spend some 10^7 to 10^8 yr in the MS phase (MM2000), so they can be considered as evolving at a nearly constant mass regime. Although the mass-loss rates currently assumed for stars in the $12 \lesssim M/M_\odot \lesssim 25$ mass interval are higher than quoted above, they cannot account for a total loss of the order of $\sim 10\ M_\odot$ during the MS phase to explain the slope of the upper edge of

the strip of points in Fig. 6 in terms of a drift towards the less massive side as the stars evolve from ZAMS to TAMS.

The right-hand slope of the lower edge of the trend in Fig. 6b may suggest that B stars of low mass need to spend some mass-dependent time in the MS before they can display the Be phenomenon; i.e. the time needed for the surface velocity be spun up to $\Omega/\Omega_\mathrm{c} \sim 0.9$.

We can also speculate on the tilted aspect of the distribution of points in Fig. 6b as produced by a mass-dependent distribution of initial equatorial velocities in the ZAMS, i.e. that massive stars start their MS phase with higher average rotational velocities than the less massive ones relative to the respective critical velocities. While the suggestion of a mass-dependent evolution of surface rotational velocities needs a thorough theoretical study, some clues on the initial rotation in the ZAMS can be obtained from the basics of stellar structure and correlations drawn from observations.

Evolutionary models of rotating stars (Meynet & Maeder 2000, 2002) suggest that we can divide the interior of stars in the ZAMS roughly into two regions, *core* and *envelope*, which rotate each at different, but respectively at near uniform angular velocities. The total stellar angular momentum J can then be written as:

$$\left.\begin{aligned} J &= k_\mathrm{co}M_\mathrm{co}R_\mathrm{co}^2\Omega_\mathrm{co} + k_\mathrm{E}(M_* - M_\mathrm{co})(R^2 - R_\mathrm{co}^2)\Omega_\mathrm{E} \\ &= k_\mathrm{E}M_*R^2\Omega_\mathrm{E} \times f \end{aligned}\right\} \qquad (8)$$

where the k_co and k_E are the gyration radii; M_co and M_E are the masses; R_co and R_E the radii; Ω_co and Ω_E are the angular velocities of the *core* and *envelope* respectively; "*" stands for the whole star. To obtain from (8) an insight on the mass dependence of the initial velocity V_o, let us note that in MM2000 models we have $M_\mathrm{co}/M_* \lesssim 0.4$, $R_\mathrm{co}/M_* \lesssim 0.4$, $\Omega_\mathrm{co}/\Omega_\mathrm{E} \lesssim 3$. Moreover, assuming that $k_\mathrm{co} \sim 0.132$ and $k_\mathrm{e} \sim 0.04$ as it would correspond to "average" polytropes of indices $n = 1.5$ for the convective core and $n = 3.0$ for the radiative envelope, we obtain that f in relation (8) is fairly independent of mass and $f \sim 1$.

On the other hand, using observed $V \sin i$ values Kawaler (1987) has shown that on average the angular momentum of dwarfs depends on the stellar mass as:

$$J \sim M_*^{2.0}. \qquad (9)$$

Since the initial MS radii of stars R_o scale with the stellar mass as:

$$R_\mathrm{o} \sim M_*^{0.6} \qquad (M_* \gtrsim 2\ M_\odot), \qquad (10)$$

from (9) for $R = R_\mathrm{o}$ the ratio of the average initial equatorial velocity of stars $V_\mathrm{o} = \Omega_\mathrm{E}R_\mathrm{o}$ normalized to the critical velocity $V_\mathrm{cr} \simeq (GM_*/1.5R_\mathrm{o})^{1/2}$ is related to the stellar mass as:

$$\frac{V_\mathrm{o}}{V_\mathrm{cr}} \sim \frac{M_*^{0.2}}{k_\mathrm{E}}. \qquad (11)$$

Knowing that for the whole range of stellar masses concerned by the Be phenomenon, models of the stellar interior in the ZAMS are homologous, it follows that the gyration radius k_E is independent of mass over the surveyed range of masses. Thus, (11) gives us a first insight into the possible initial dependence

of rotational velocities on mass, which implies that stars with masses $M_* \gtrsim 15\ M_\odot$ can have initial rotational velocities 25% closer to the critical one than those with masses $M_* \lesssim 5\ M_\odot$. This mass dependence is small indeed. However, to account entirely for the noted tendency that hot stars reach the near/or critical rotation at smaller ratios τ/τ_{MS} than the cooler ones, there must still be some interaction between rotationally and evolutionary-induced changes on the stellar moment of inertia that can be felt as due to a small mass-related decrease of the gyration radius.

Let us finally note that if we neglect the possible small mass-dependence of k_E from $M_* \sim 15\ M_\odot$ to ~5 $M_\odot$, relations (10) and (11) will imply that $V_o(15)/V_o(5) \sim 1.6$, while from observations of dwarf Be stars, which are on average at a later evolutionary stage than implied by V_o, we derive $V(15)/V(5) \sim 1.3$ (cf. Sect. 3.3). This suggests that to obtain results of the kind shown in Fig. 6b, it would be better to use models with $V_o = f(M) > 300$ km s^{-1} (cf. Sect. 3.4), rather than $V_o = 300$ km s^{-1}. Such a choice would imply the use of re-scaled evolutionary tracks. We preferred, however, to keep the original models by MM2000, since they depict the effects of fast rotation in a more consistent way and because altogether they give reliable orders of magnitude of these effects.

5.3. Comparison with model predictions

The noticeable lack of Be stars with masses $M \gtrsim 12\ M_\odot$ in the upper half of the MS can be explained as the natural result of angular momentum loss produced by mass-loss, whose rate increases with the stellar mass. This loss reduces the surface equatorial rotational velocity converting the star into a much lower rotating object ($\omega \ll 0.9$). Conversely, the increase of the number of Be stars with masses $M \lesssim 10\ M_\odot$ in the upper half of the MS must be an effect of internal coupling, where the angular momentum is conveyed from the stellar core to the surface by the meridional circulation. The time scale of the meridian circulation is roughly $\tau_{circ} \sim \tau_{KH}/\eta$ where τ_{KH} is the Kelvin-Helmholtz time and η is the ratio of the centrifugal force to the gravity. Since for Be stars it is $\eta \sim 1$, τ_{circ} ranges with the stellar mass as $\tau_{circ} \sim 4 \times 10^6 (M/M_\odot)^{-2}$ yr. It then becomes clear that the lapse of time to reach $\Omega/\Omega_c \sim 1$ is longer the smaller the stellar mass (MM2000 and Maeder 2004, private communication), similar to model predictions.

5.4. On the rotational velocities and star formation regions

From HIPPARCOS parallaxes we see that 84% of stars in our sample lie in a region within 500 pc of the Sun, of which 62% are within 300 pc. It is also noteworthy that 45% of the more massive objects of this sample, hotter than 22 000 K, are within 300 pc and 35% are between 300 and 500 pc. Only two stars are at $d \sim 800$ pc. The stellar sample studied should not then be characterized by strong differences in the initial metallicity. In fact, low metallicities might favor the fast rotation in some cases (Maeder et al. 1999), but it cannot be the case for the massive Be stars of our sample. According to

Meynet & Maeder (2002) low metallicity reduces the mass-loss rate, which favors the conservation of angular momentum in the stellar surface and so, the existence of higher surface rotational velocities. Also, Maeder & Meynet (2001) predict that the increase of the Ω/Ω_c ratio towards 1 in massive stars is faster in models with low metallicity. It would then be interesting to test this prediction by obtaining diagrams like those in Fig. 6 for Be stars in environments with quite different metal abundance, an aim that we will pursue in subsequent work.

5.5. On the initial conditions

The calculated properties of an evolving object with rotation in the MS depend on the assumed initial conditions. The results given in the present work depend on predictions made for stars which began evolving in the ZAMS as rigid rotators. This choice may, however, be not the only possible. Similarly to ZAMS, which is likely a computational "landmark" (Endal & Sofia 1981), rigid rotation in the ZAMS may be a simplification too. On the one hand, the necessity and/or definition of a ZAMS for massive stars is not clear, as it happens in the accretion paradigm of star formation (Palla & Stahler 1993; Beech & Mitalas 1994; Maeder & Behrend 2002). On the other hand, due to hydrodynamical instabilities, an initial rigid rotation switches rapidly (some 10^4 yr) into a differential rotation (Denissenkov et al. 1999; Meynet & Maeder 2000). Such a differential rotation may then be present before the "ZAMS" phase.

In the classical PMS evolution frame, based on the contraction of a constant mass sphere until the gravitational energy release increases the central temperature enough to trigger the nuclear reactions, rigid rotation in the ZAMS was generally justified because: a) dynamical stability against axisymmetric perturbations could be warranted for rigid stellar rotators (Fujimoto 1987); b) it was assumed that in the PMS the full convection phase stars become rigid rotators. However, recent 2D hydrodynamical calculations show that convection does not maintain rigid rotation, but it rather produces an internal angular velocity distribution profile $\Omega(\varpi) \propto \varpi^{-p}$ (ϖ = distance to the rotation axis), which is intermediate between complete redistribution of specific angular momentum ($p = 2$) and rigid rotation ($p = 0$) (Deupree 1998, 2000, 2001). Furthermore, in the accretion formation scheme the star is a mass and angular momentum gaining object (Palla & Stahler 1993; Mercer-Smith et al. 1999; Terebey et al. 1984). Meanwhile a non-rotating star gains mass, it first undergoes a full-convection period, then a radiative core is developed, the star swells until a temporary full radiative state is attained and finally the core becomes convective. During this period the forming star stretches and contracts, but it can also undergo magnetic interaction with the accretion disc (Stępień 2002). These phenomena can produce an uneven distribution of the angular momentum inside the star. There is also some decoupling of stellar internal regions, since the time scales of angular momentum redistribution in convective and radiative zones are different (Endal & Sofia 1981). If the star acquires mass

through an accretion disc, which is probably in Keplerian rotation, a huge gain of angular must take place (Packet 1981):

$$\dot{J}(t) \approx [GR(t)M(t)]^{1/2}\dot{M}(t) \qquad (12)$$

where G is the gravitional constant, R and M are the time-dependent radius and mass of the star respectively and $\dot{M}$ is the mass accretion rate [$\dot{M} \sim 10^{-5}(M/M_\odot)^\phi \ M_\odot$/yr with $\phi \sim 1.0{-}1.5$ (Maeder & Behrend 2002)]. Since the rigid rotation implies a very low amount of rotational energy, it cannot be then excluded that a considerable load of angular momentum may exist somewhere deep inside the star, so that an a priori assumption of rigid rotation can be difficult to justify. However, it was noticed by Spruit (1999, 2002) that a powerful enough differential rotation can create magnetic fields. Different regions inside the star could then be "locked" to recover some degree of rigid rotation (Maeder & Meynet 2003).

Stępień (2002) has suggested that given an appropriate range of surface magnetic fields, stars may gain angular momentum through an effective magnetic accretion in the PMS phase. Stępień (2002) notes that the rotation can be faster the more massive the star, because the interaction with the circumstellar matter lasts less time. Nevertheless, the final balance between losses and gains of angular momentum produced by interactions with the circumstellar environment were not definitively established, nor were its consequences on the internal rotation law of the star. In particular, very little was said about the amount of rotational kinetic energy the star is left with after these interactions.

Rigid rotation puts an upper limit onto the amount of rotational kinetic energy $\mathcal{K}$ a star can store. At rigid critical rotation, an early-type star has $\mathcal{E}_c = \mathcal{K}_c/|\mathcal{W}| \simeq 0.015$ ($\mathcal{W}$ = gravitational potential energy). In a star with internal differential rotation, the same surface rotations may correspond to higher values of $\mathcal{E}$, which may then carry stronger stellar deformations, gravity darkening effects and internal hydrodynamical instabilities. For an order of magnitude estimate, Table 4 gives the rotational kinetic energy ratios $\mathcal{K}(p)/\mathcal{K}(p=0)$ and energy ratios $\mathcal{E}(p) = \mathcal{K}(p)/|\mathcal{W}(p)|$ for an internal rotational law $\Omega(\varpi) \propto \varpi^{-p}$, assuming that the stellar surface rotates at $\Omega_s/\Omega_c = 0.9$ as occurs on average for Be stars. These values were obtained using two dimentional models of stellar structure (Zorec et al. 1988a). We see that for a mild differential rotation $p = 0.4$ it is $\mathcal{E} > \mathcal{E}_c$ and that for $p = 0.7$, an average rotation law set by convection, $\mathcal{E}$ is nearly twice as high as for a critical rigid rotator. In such a case there is a lowering of the core bolometric luminosity that ranges from roughly 17% at masses $M \sim 30 \ M_\odot$ to 27% in masses $M \sim 3 \ M_\odot$ (Clement 1979). A much complicate relation must then exist between spectra, masses and stellar ages than treated in the present work (Collins & Smith 1985; Zorec 1986; Zorec et al. 1987, 1988b,a, 1990; Zorec 1992).

6. Conclusions

In this paper we have studied a sample of 97 field Be stars, most of which are at distances $d < 500$ pc from the Sun, so that they can be considered more or less homogeneous regarding their initial metallicity. All these stars were observed in the

Table 4. Kinetic energy ratios and $\mathcal{E}$ ratios calculated for different values of p.

p	$\mathcal{K}(p)/\mathcal{K}(p=0)$	$\mathcal{E}(p)$
0.4	1.52	0.018
0.7	2.17	0.026
1.0	3.26	0.038

BCD spectrophotometric system to have photospheric spectral signatures as much as possible free of CE emission/absorption perturbations. The apparent fundamental parameters derived from the observed BCD (λ_1, D) quantities, i.e. parameters reflecting the average rotationally-perturbed photosphere shown by the projected stellar hemisphere towards the observer, were translated into *pnrc* and *averaged* fundamental parameters. "*pnrc*" is the acronym for *parent non-rotating counterparts*, or parameters that correspond to homologous non-rotating stars. The *averaged* fundamental parameters correspond to averages over the whole stellar surface. We have assumed that the studied Be stars rotate with an angular velocity ratio $\Omega/\Omega_c = 0.88$ (Frémat et al. 2005). Note the difference between *averaged* and *apparent*, the last representing a sort of average spectrum emitted by the "observed" stellar hemisphere. The *averaged* parameters are the only quantities that can be used to interpolate stellar masses and ages in the evolutionary tracks.

The present contribution represents one of the first attempts to derive stellar masses and ages of Be stars by using simultaneously model atmospheres and evolutionary tracks both calculated for rotating objects. According to the statistical average of true rotational velocities V of dwarf Be stars, the evolutionary models used are for ZAMS equatorial rotational velocity $V_o = 300$ km s^{-1} in all masses. For all stars we derived the mass and stellar ages τ normalized to the respective time that each rotating star can spend in the main sequence phase τ_{MS}. As a consequence of effects of the rapid rotation described by the models used, we obtained a trend of points in the $(\tau/\tau_{MS}, M/M_\odot)$ diagram, which implies that:

a) there are Be stars spread over the whole age interval $0 \lesssim \tau/\tau_{MS} \lesssim 1$ in the main sequence evolutionary phase;

b) in massive stars the Be phenomenon tends to be present at lower τ/τ_{MS} age ratios than in the less massive stars.

The lack of massive stars in the upper MS can be due to loss of angular momentum through mass-loss which produces a strong decrease of the stellar surface Ω/Ω_c ratio. On the other hand, the increase of the number of less massive Be stars in the upper MS can be explained in terms of angular momentum transport from the core to the surface carried by the meridional circulation, which has longer time scales the lower the stellar mass.

Arguments based on the distribution of the total angular momentum of dwarf stars against mass reveal that the massive stars may start evolving from the ZAMS with a slightly higher V_o/V_c than the less massive ones.

References

Baillet, A., Chalonge, D., & Divan, L. 1973, Nouv. Rev. Opt., 4, 151

Beech, M., & Mitalas, R. 1994, ApJS, 95, 517

Behrend, R., & Maeder, A. 2001, A&A, 373, 190

Bodenheimer, P. 1971, ApJ, 167, 153

Chalonge, D., & Divan, L. 1952, Ann. Astrophys., 15, 201

Chauville, J., Zorec, J., Ballereau, D., et al. 2001, A&A, 378, 861

Cidale, L., Zorec, J., & Morrell, N. 2000, ASPC, 214, 87

Cidale, L., Zorec, J., & Tringaniello, L. 2001, A&A, 368, 160

Claret, A. 1998, A&A, 335, 647

Clement, M. J. 1979, ApJ, 230, 230

Coe, M. J. 2000, in IAU Colloq., 175, The Be Phenomenon in Early-Type Stars, ASP Conf. Ser., 214, 656

Collins, G. W., & Smith, R. C. 1985, MNRAS, 213, 519

Collins, G. W., & Sonneborn, G. H. 1977, ApJS, 34, 41

Collins, G. W., & Truax, R. J. 1995, ApJ, 439, 860

Collins, G. W., Truax, R. J., & Cranmer, S. R. 1991, ApJS, 77, 541

Crampin, J., & Hoyle, F. 1960, MNRAS, 120, 33

Denissenkov, P. A., Ivanova, N. S., & Weiss, A. 1999, A&A, 341, 181

Deupree, R. G. 1998, ApJ, 499, 340

Deupree, R. G. 2000, ApJ, 543, 395

Deupree, R. G. 2001, ApJ, 552, 268

Divan, L., & Zorec, J. 1982, The Scientific Aspects of the Hipparcos Space Astrometry Mission, ESA SP-177, 101

Endal, A. S. 1982, in Be Stars, IAU Symp., 98, 299

Endal, A. S., & Sofia, S. 1979, ApJ, 232, 531

Endal, A. S., & Sofia, S. 1981, ApJ, 243, 625

Fabregat, J., & Torrejón, J. M. 2000, A&A, 357, 451

Feinstein, A. 1990, Rev Mex. Astron. Astrofis., 21, 373

Frémat, Y., Zorec, J., Hubert, A.-M., & Floquet, M. 2005, A&A, submitted

Fujimoto, M. Y. 1987, A&A, 176, 53

Gies, D. R. 2000, in IAU Colloq., 175, The Be Phenomenon in Early-Type Stars, ASP Conf. Ser., 214, 668

Hardorp, J., & Strittmatter, P. A. 1970, in Stellar Rotation, IAU Colloq., 4, 48

Harmanec, P. 1987, in Physics of Be Stars, IAU Colloq., 92, 339

Heger, A., & Langer, N. 2000, ApJ, 544, 1016

Hubert, A. M., Floquet, M., & Zorec, J. 2000, in IAU Colloq., 175, The Be Phenomenon in Early-Type Stars, ASP Conf. Ser., 214, 348

Hubert-Delplace, A. M., Hubert, H., Chambon, M. T., & Jaschek, M. 1982, in Be Stars, IAU Symp., 98, 125

Jaschek, M., Jaschek, C., Hubert-Delplace, A.-M., & Hubert, H. 1980, A&AS, 42, 103

Jaschek, M., Slettebak, A., & Jaschek, C. 1981, Be Stars Newsl., No. 4, 9

Kawaler, S. D. 1987, PASP, 99, 1322

Maeder, A., & Behrend, R. 2002, ASPC, 267, 179

Maeder, A., & Meynet, G. 2001, A&A, 373, 555

Maeder, A., & Meynet, G. 2003, A&A, 411, 543

Maeder, A., & Peytremann, E. 1970, A&A, 7, 120

Maeder, A., & Peytremann, E. 1972, A&A, 21, 279

Maeder, A., Grebel, E. K., & Mermilliod, J. 1999, A&A, 346, 459

Massa, D. 1975, PASP, 87, 777

Mercer-Smith, J. A., Cameron, A. G. W., & Epstein, R. I. 1984, ApJ, 279, 363

Mermilliod, J. C. 1982, A&A, 109, 48

Meynet, G., & Maeder, A. 2000, A&A, 361, 101 (MM2000)

Meynet, G., & Maeder, A. 2002, A&A, 390, 561

Moss, D., & Smith, R. C. 1982, Rep. Progr. Phys., 44, 831

Moujtahid, A., Zorec, J., & Hubert, A. M. 1999, A&A, 349, 151

Moujtahid, A., Zorec, J., Hubert, A. M., Garcia, A., & Burki, G. 1998, A&AS, 129, 289

Owocki, S. P. 2004, in Stellar Rotation, ed. A. Maeder, & Ph. Eenens (ASP Conf. Ser. & IAU Publ.), IAU Symp., 215, 515

Packet, W. 1981, A&A, 102, 17

Palla, F., & Stahler, S. W. 1993, ApJ, 418, 414

Pols, O. R., Cote, J., Waters, L. B. F. M., & Heise, J. 1991, A&A, 241, 419

Sackmann, I. J. 1970, A&A, 8, 76

Schaller, G., Schaerer, D., Meynet, G., & Maeder, A. 1992, A&AS, 96, 269

Schild, R., & Romanishin, W. 1976, ApJ, 204, 493

Schmidt-Kaler, T. 1964, Veroeffentlichungen des Astronomisches Institute der Universitaet Bonn, 70, 1

Slettebak, A. 1979, Space Science Rev., 23, 541

Slettebak, A. 1985, ApJS, 59, 769

Slettebak, A., Kuzma, T. J., & Collins, G. W. 1980, ApJ, 242, 171

Spruit, H. C. 1999, A&A, 349, 189

Spruit, H. C. 2002, A&A, 381, 923

Stępień, K. 2002, A&A, 383, 218

Stoeckley, T. R. 1968, MNRAS, 140, 141

Stoeckley, T. R., & Mihalas, D. 1973, Limb darkening and rotation broadening of He I and Mg II line profiles in early-type stars, NCAR-TN/STR-84

Struve, O. 1931, ApJ, 73, 94

Talon, S., Zahn, J.-P., Maeder, A., & Meynet, G. 1997, A&A, 322, 209

Tassoul, J. 1978, Theory of rotating stars (Princeton Series in Astrophysics, Princeton: University Press)

Terebey, S., Shu, F. H., & Cassen, P. 1984, ApJ, 286, 529

Townsend, R. H. D., Owocki, S. P., & Howarth, I. D. 2004, MNRAS, 350, 189

van Bever, J., & Vanbeveren, D. 1997, A&A, 322, 116

von Zeipel, H. 1924a, MNRAS, 84, 665

von Zeipel, H. 1924b, MNRAS, 84, 684

Wolff, S. C., Strom, S. E., & Hillenbrand, L. A. 2004, ApJ, 601, 979

Zorec, J. 1986, Thèse d'État Paris: Université VII

Zorec, J. 1992, Hipparcos: Une nouvelle donne pour l'Astronomie (Observatoire de la Côte d'Azur & Société française des Spécialistes d'Astronomie), 407

Zorec, J. 2004, in Stellar Rotation, ed. A. Maeder, & Ph. Eenens (ASP Conf. Ser. & IAU Publ.), IAU Symp., 215, 73

Zorec, J., & Briot, D. 1991, A&A, 245, 150

Zorec, J., & Briot, D. 1997, A&A, 318, 443

Zorec, J., Divan, L., Mochkovitch, R., & Garcia, A. 1987, in Physics of Be Stars, IAU Colloq., 92, 68

Zorec, J., Mochkovitch, R., & Divan, L. 1988a, Académie des Sciences Paris Comptes Rendus Série Sciences Mathématiques, 306, 1265

Zorec, J., Mochkovitch, R., & Garcia, A. 1988b, Académie des Sciences Paris Comptes Rendus Série Sciences Mathématiques, 306, 1225

Zorec, J., Mochkovitch, R. A., & Garcia, A. 1990, in NATO ASIC Proc., 316: Angular Momentum and Mass Loss for Hot Stars, 239

Zorec, J., Frémat, Y., Hubert, A. M., & Floquet, M. 2002, in IAU Colloq., 185: Radial and Nonradial Pulsations as Probes of Stellar Physics, ASP Conf. Ser., 259, 244

Zorec, J., Levenhagen, R., Chauville, J., et al. 2004, in Stellar Rotation, ed. A. Maeder, & Ph. Eenens (ASP Conf. Ser. & IAU Publ.), IAU Symp., 215, 89

Online Material

Table 1. Program stars, observed and derived parameters.

HD	D	λ_1	$T_{\rm eff}$	$\log g$	$V\sin i$	$\overline{T}_{\rm eff}$	$\log \overline{g}$	$M/M_\odot$	$\log \tau$	$\tau/\tau_{\rm MS}$	$M/M_\odot$	$\log \tau$	$\tau/\tau_{\rm MS}$
	dex	Å	K	dex	km s^{-1}	K	dex		τ(yr)			τ(yr)	
			Apparent			Averaged		$\Omega/\Omega_{\rm c} = 0$			$\Omega/\Omega_{\rm c} = 0.88$		
4180	0.269	41.2	14 400	3.36	195	14 800	3.48	5.7	7.85	1.01	6.0	7.87	0.96
5394	0.062	66.2	28 670	4.20	432	30 240	4.06	14.3	6.81	0.53	16.1	6.64	0.32
10144	0.241	39.9	15 040	3.48	235	16 090	3.47	6.2	7.76	1.02	6.7	7.74	0.96
10516	0.079	61.3	26 540	4.20	440	28 760	4.18	11.7	6.85	0.42	13.8	6.28	0.12
20336	0.179	59.4	18 720	4.20	328	19 620	4.10	6.4	7.46	0.56	7.1	7.20	0.31
22192	0.230	45.0	15 670	3.69	275	16 840	3.62	6.2	7.74	0.97	6.7	7.70	0.88
23016	0.377	43.1	12 130	3.71	235	12 790	3.74	4.0	8.16	0.91	4.3	8.13	0.79
23302	0.343	40.4	12 460	3.44	170	13 010	3.57	4.6	8.08	1.01	4.7	8.08	0.92
23480	0.299	44.6	13 620	3.69	240	14 190	3.69	4.8	7.97	0.93	5.0	7.97	0.83
23630	0.363	31.9	12 260	3.05	140	12 410	3.06	6.1	7.78	1.02	5.9	7.91	1.02
23862	0.381	53.1	12 100	3.98	290	12 890	4.03	3.4	8.20	0.66	3.8	8.01	0.45
24534	0.062	59.9	28 120	4.20	293	28 140	3.96	14.3	6.88	0.62	14.3	6.89	0.50
25940	0.228	48.2	16 180	3.82	197	16 720	3.79	6.0	7.73	0.89	6.1	7.72	0.73
28497	0.063	55.9	28 090	4.08	342	28 970	4.13	13.3	6.79	0.45	14.3	6.52	0.21
30076	0.129	46.8	21 410	3.85	213	21 960	3.87	9.1	7.32	0.82	9.3	7.29	0.65
32343	0.235	59.5	16 100	4.11	95	15 460	4.02	5.2	7.74	0.63	5.0	7.73	0.47
35411	0.126	98.3	22 690	4.19	170	21 970	3.88	9.7	7.23	0.73	9.3	7.29	0.64
35439	0.134	52.5	22 300	3.98	263	22 800	3.98	9.1	7.25	0.69	9.5	7.16	0.49
36576	0.122	53.7	22 880	4.02	265	23 660	3.90	10.1	7.22	0.76	10.4	7.16	0.63
37202	0.155	44.2	19 610	3.74	310	20 050	3.68	8.5	7.42	0.89	8.6	7.46	0.81
37490	0.163	48.3	20 100	3.51	172	19 000	3.44	8.4	7.45	0.91	8.1	7.53	0.83
37657	0.195	48.0	17 530	3.76	198	17 870	3.77	6.8	7.60	0.89	6.9	7.62	0.76
37795	0.326	43.0	12 810	3.64	180	13 140	3.64	4.6	8.05	0.96	4.6	8.08	0.87
37967	0.239	55.0	15 900	4.02	210	15 920	3.93	5.3	7.78	0.74	5.4	7.75	0.59
38010	0.069	58.0	27 480	4.19	370	28 470	4.28	11.8	6.37	0.14	13.0	5.35	0.01
40978	0.180	61.5	18 430	3.77	200	19 020	3.81	7.3	7.53	0.86	7.5	7.52	0.71
41335	0.129	51.0	21 800	3.92	358	23 650	4.02	8.7	7.28	0.68	10.1	7.07	0.44
42545	0.238	56.0	15 600	4.08	285	16 110	3.97	5.1	7.81	0.72	5.4	7.71	0.54
44458	0.086	44.0	23 870	3.55	242	24 570	3.63	12.9	7.11	0.91	12.9	7.16	0.83
45314	0.040	55.2	30 630	4.04	285	30 620	4.08	16.2	6.65	0.43	16.5	6.58	0.28
45542	0.300	46.0	13 480	3.68	217	14 100	3.73	4.7	7.99	0.92	4.9	7.99	0.80
45725	0.192	55.0	18 070	4.06	330	18 940	3.95	6.5	7.58	0.73	7.0	7.47	0.56
45910	0.078	32.2	20 660	2.74	240	22 320	2.77	22.1	6.84	1.01	23.3	6.92	1.01
45995	0.120	51.7	22 440	3.94	255	22 570	3.82	9.9	7.25	0.79	9.9	7.27	0.68
47054	0.361	43.1	12 490	3.68	219	13 090	3.70	4.3	8.10	0.94	4.5	8.09	0.83
50013	0.092	87.9	26 380	4.20	243	25 800	4.12	11.5	6.81	0.37	11.4	6.73	0.25
50083	0.124	48.0	21 930	3.85	170	22 500	3.77	10.1	7.26	0.87	10.1	7.28	0.73
53974	0.054	51.0	28 910	3.84	100	27 810	3.69	18.1	6.85	0.80	16.1	7.01	0.77
56014	0.169	37.8	18 540	3.29	280	20 330	3.34	9.8	7.36	1.02	10.7	7.36	0.98
56139	0.190	55.6	18 110	4.05	85	17 360	3.87	6.6	7.58	0.77	6.3	7.64	0.66
57219	0.218	46.5	16 500	3.81	80	15 850	3.71	6.2	7.70	0.89	5.9	7.80	0.81
58050	0.162	60.2	20 100	4.20	130	19 360	4.02	7.3	7.37	0.59	7.1	7.36	0.45
58343	0.230	48.0	16 250	3.79	43	15 520	3.73	6.1	7.72	0.89	5.7	7.84	0.80
58715	0.400	50.9	11 740	3.88	230	12 060	3.94	3.5	8.26	0.75	3.6	8.18	0.58
60848	0.051	71.1	29 930	4.20	247	30 760	4.33	14.2	6.22	0.13	14.9	...	0.00
63462	0.050	78.0	30 020	4.20	435	32 020	4.04	16.4	6.78	0.58	18.5	6.60	0.35

Table 1. continued.

HD	D	λ_1	T_{eff}	$\log g$	$V\sin i$	$\overline{T}_{eff}$	$\log \overline{g}$	$M/M_\odot$	$\log \tau$	τ/τ_{MS}	$M/M_\odot$	$\log \tau$	τ/τ_{MS}
65875	0.142	54.0	21 350	4.04	153	20 670	3.92	8.5	7.32	0.69	8.2	7.36	0.58
68980	0.072	57.7	26 800	4.20	145	25 840	4.08	12.0	6.84	0.44	11.6	6.82	0.34
83953	0.253	49.7	14 800	3.78	260	15 650	3.81	5.1	7.88	0.86	5.5	7.82	0.72
91120	0.438	50.0	10 780	3.95	307	11 950	3.92	3.2	8.38	0.81	3.6	8.21	0.61
91465	0.193	43.0	17 200	3.63	266	18 630	3.66	7.1	7.60	0.96	7.7	7.56	0.82
109387	0.288	45.0	14 174	3.59	200	14 670	3.69	5.2	7.91	0.93	5.3	7.92	0.83
110432	0.150	80.0	20 350	3.92	400	22 510	3.90	8.1	7.40	0.76	9.6	7.24	0.61
112091	0.151	63.0	21 190	4.05	210	21 600	4.27	7.5	7.04	0.28	7.9	6.21	0.04
120324	0.112	54.4	23 130	4.04	159	22 410	3.95	9.6	7.18	0.65	9.3	7.22	0.55
120991	0.106	53.3	23 320	3.95	70	22 330	3.82	10.5	7.19	0.76	9.8	7.29	0.69
124367	0.222	57.8	16 460	4.04	295	17 060	4.08	5.2	7.68	0.57	5.7	7.48	0.36
127972	0.165	51.4	20 050	3.94	310	20 730	3.92	7.6	7.41	0.71	8.2	7.35	0.57
131492	0.145	57.8	21 120	4.09	185	20 560	3.99	8.0	7.31	0.68	7.9	7.31	0.48
135734	0.356	54.5	12 580	4.06	278	13 290	4.06	3.6	8.14	0.66	4.0	7.94	0.42
137387	0.134	69.1	21 980	4.20	250	21 949	4.13	8.2	7.15	0.44	8.5	6.96	0.24
138749	0.278	52.6	14 440	3.84	340	15 969	3.96	4.6	7.93	0.73	5.4	7.73	0.55
142184	0.140	65.6	21 540	4.20	340	22 790	4.30	7.6	6.93	0.23	8.6	5.68	0.01
142926	0.383	54.0	12 060	3.98	336	13 320	4.08	3.4	8.20	0.63	4.0	7.89	0.37
142983	0.200	48.0	17 790	3.80	390	20 240	3.93	6.4	7.60	0.77	7.9	7.38	0.56
148184	0.046	66.3	30 700	4.20	144	29 590	4.14	15.6	6.47	0.27	14.9	6.42	0.17
149438	0.061	51.5	28 600	3.83	15	27 310	3.85	15.6	6.88	0.69	14.1	7.00	0.64
149757	0.068	60.2	27 810	4.20	348	28 610	4.01	13.8	6.89	0.60	14.5	6.81	0.42
157042	0.129	57.8	22 050	4.19	340	22 560	4.11	8.3	7.16	0.46	9.0	6.97	0.29
158427	0.201	58.6	17 360	4.13	290	17 780	4.04	5.8	7.61	0.60	6.2	7.48	0.43
162732	0.312	49.3	13 070	3.81	310	14 120	3.80	4.3	8.07	0.86	4.8	7.98	0.74
164284	0.141	62.6	21 650	4.11	280	21 830	3.98	8.2	7.23	0.52	8.5	7.08	0.33
173948	0.123	46.8	22 250	3.83	140	21 550	3.59	11.2	7.21	0.91	10.4	7.33	0.85
174237	0.198	56.0	17 450	4.07	163	16 960	3.83	6.4	7.63	0.81	6.2	7.69	0.70
178175	0.157	37.6	18 940	3.49	105	18 290	3.50	8.7	7.44	0.99	8.2	7.55	0.91
183656	0.288	35.0	12 630	3.29	275	14 110	3.30	5.3	7.92	1.02	5.9	7.90	1.02
184915	0.060	47.4	27 830	3.60	229	28 190	3.67	17.5	6.90	0.84	16.9	6.99	0.77
187811	0.190	53.0	17 790	3.93	245	18 600	4.00	6.3	7.60	0.72	6.7	7.45	0.48
192044	0.319	44.4	12 940	3.66	245	13 770	3.67	4.6	8.03	0.95	4.9	8.01	0.85
194335	0.133	70.9	22 200	4.20	360	22 970	4.23	8.1	6.90	0.23	8.9	6.40	0.07
200120	0.124	65.7	22 650	4.20	379	23 870	4.10	8.9	7.16	0.53	10.0	6.90	0.29
202904	0.162	57.8	20 470	4.06	185	20 460	4.08	7.5	7.34	0.57	7.7	7.20	0.35
203374	0.055	67.5	29 130	4.20	333	29 830	3.88	16.6	6.85	0.71	16.9	6.87	0.58
205637	0.175	38.5	17 880	3.19	225	19 070	3.40	8.7	7.45	1.02	9.2	7.48	0.97
206773	0.050	65.3	30 460	4.20	390	31 500	4.16	15.6	6.59	0.35	17.0	6.21	0.12
209014	0.366	53.4	12 360	3.87	320	13 350	3.84	3.8	8.17	0.81	4.3	8.06	0.69
209409	0.333	48.0	12 770	3.81	280	13 960	3.87	4.1	8.11	0.85	4.6	7.98	0.66
209522	0.228	46.1	16 260	3.80	275	17 020	3.76	6.0	7.72	0.86	6.4	7.69	0.77
210129	0.300	44.4	13 390	3.62	130	13 770	3.70	4.9	7.98	0.96	4.8	8.02	0.83
212076	0.093	48.3	24 290	3.81	98	23 340	3.82	11.3	7.13	0.76	10.6	7.22	0.68
212571	0.076	57.0	27 020	4.19	230	27 770	4.13	12.6	6.90	0.54	13.1	6.57	0.21
214748	0.385	38.0	11 999	3.45	200	12 400	3.46	4.4	8.12	1.02	4.6	8.14	0.98
217050	0.186	40.4	17 660	3.54	340	20 180	3.59	7.7	7.55	0.98	9.2	7.43	0.88
217543	0.208	52.5	16 990	3.85	330	18 610	3.95	5.9	7.68	0.76	6.8	7.49	0.55
217675	0.281	38.3	14 140	3.17	292	15 800	3.34	6.0	7.78	1.02	6.8	7.74	1.01
217891	0.286	51.3	14 050	3.84	95	13 530	3.83	4.6	7.97	0.82	4.4	8.04	0.71
224686	0.419	44.5	11 320	3.76	300	12 260	3.75	3.6	8.28	0.89	4.0	8.20	0.78